Available online at www.sciencedirect.com
ScienceDirect
Procedia Engineering 2 (2010) 1915–1925
Procedia Engineering
www.elsevier.com/locate/procedia

Fatigue 2010

Microstructural effects on fatigue crack growth behavior of a microalloyed steel

D.F. Laurito[a], C.A.R.P. Baptista[a]*, M. A. S. Torres[b], A. J. Abdalla[c]

[a]*Department of Materials Engineering, Escola de Engenharia de Lorena, University of São Paulo, Lorena/SP, Brazil*
[b]*Department of Mechanics, FEG/UNESP, São Paulo State University, Guaratinguetá/SP, Brazil*
[c]*IEAv/CTA – Instituto de Estudos Avançados, Comando-Geral de Tecnologia Aeroespacial São José dos Campos/SP, Brazil*

Received 8 March 2010; revised 10 March 2010; accepted 15 March 2010

Abstract

Thermal transformations on microalloyed steels can produce multiphase microstructures with different amounts of ferrite, martensite, bainite and retained austenite. These different phases, with distinct morphologies, are determinant of the mechanical behavior of the steel and can, for instance, affect the crack path or promote crack shielding, thus resulting in changes on its propagation rate under cyclic loading. The aim of the present work is to evaluate the effects of microstructure on the tensile strength and fatigue crack growth (FCG) behaviour of a 0.08%C-1,5%Mn (wt. pct.) microalloyed steel, recently developed by a Brazilian steel maker under the designation of RD480. This steel is being considered as a promising alternative to replace low carbon steel in wheel components for the automotive industry. Various microstructural conditions were obtained by means of heat treatments followed by water quench, in which the material samples were kept at the temperatures of 800, 950 and 1200°C. In order to describe the FCG behavior, two models were tested: the conventional Paris equation and a new exponential equation developed for materials showing non-linear FCG behavior. The results allowed correlating the tensile properties and crack growth resistance to the microstructural features. It is also shown that the Region II FCG curves of the dual and multiphase microstructural conditions present crack growth transitions that are better modeled by dividing them in two parts. The fracture surfaces of the fatigued samples were observed via scanning electron microscopy in order to reveal the fracture mechanisms presented by the various material conditions.

Keywords: microalloyed steels; fatigue crack growth; heat treatment; microstructural analysis.

1. Introduction

The need for reduction of the vehicles' weight leads to the development of steels with improved chemical composition and microstructure. Thus, there is a strong drive in the steel industry to enhance the performance of the existing products, particularly, formability and toughness [1]. The mechanical properties of these new materials, which include the high strength and low alloy (HSLA) steels and the microalloyed steels, are more favourable both to manufacturing and service performance of automotive components. These steels have low or medium carbon

* Corresponding author. Tel.: +55-12-3159-9914; fax: +55-12-3153-3006.
E-mail address: baptista@demar.eel.usp.br.

1877-7058 © 2010 Published by Elsevier Ltd.
doi:10.1016/j.proeng.2010.03.206

content and small additions of alloy elements such as Mn, Nb, Mo, V and Ti. A variety of microstructures in microalloyed steels can be obtained depending on the deformation temperature, cooling rate and the chemical composition [2-4]. Accelerated cooling is one of the methods to strengthen the steels with minimum alloying content and to obtain good toughness [5]. Microalloying elements are added mainly to control the austenitic grain size of the reheating, to retard the recrystallization of austenite and to promote precipitation hardening. Elements such as Nb and Ti facilitate grain refinement by means of the precipitation and anchoring of solute in austenite and contribute to increase the strength by precipitation in ferrite during and after the austenite→ferrite transformation [6]. The improvement in the properties of microalloyed steels is primarily a consequence of fine ferrite grain size produced by the transformation of austenite [7].

On the other hand, the research involving the transformation of phases by means of inter-critical and isothermal heat treatments has intensified, with promising results given by the dual phase steels [8]. These are characterized by microstructures consisting of a dispersion of hard martensite particles in a soft ferrite matrix [9]. Many studies [9-10] have shown that martensite content is dominant in controlling tensile properties and that increasing the amount of martensite decreases ductility. Other factors that have been reported to influence the ductility of dual phase steels include the composition of the martensite, alloy content of the ferrite, retained austenite [10]. Due to its combination of high strength, good ductility and continuous yielding, dual phase steels have been considered to be ideal for the production of automobile components that require good formability [11]. Microalloyed steels can also be heat treated in order to obtain dual phase and multiphase microstructures.

The strength, ductility and fatigue resistance of steels can be related to their microstructural aspects. Tayanç *et al.* [12] investigated the effect of carbon content and martensite volume fraction on the fatigue behavior strength of dual phase steels with carbon content between 0.085% and 0.3% (wt. pct.). They observed that dual phase steels show better fatigue properties than the as received steels. Moreover, an optimum heat treatment temperature preceding water quenching was found to exist for the studied steels, with respect to tensile strength. Baptista *et al.* [13] investigated the fatigue crack growth (FCG) behavior of low carbon dual phase steels and found that a higher tensile strength corresponds to lower FCG resistance. Suzuki and McEvily [14] obtained FCG curves for dual phase steels presenting duplex microstructures with distinct phase morphologies. They observed that not only the martensite fraction volume, but also its morphology, can significantly affect the FCG behavior.

The aim of the present work was to evaluate the effects of microstructure on the fatigue crack growth behaviour of a 0.08%C-1,5%Mn (wt. pct.) microalloyed steel, recently developed by a brazilian company (CSN) under the designation of RD480. This steel is being considered as a promising alternative to replace a low carbon steel in wheel components for the automotive industry. Distinct microstructural conditions were obtained by means of inter-critical and isothermal heat treatments followed by water quench, in which the material samples were kept at the temperatures of 800, 950 and 1200°C. The effect of the microstructural changes due to these heat treatments on the tensile behaviour of this steel was object of a more detailed investigation in a previous work [15]. The as-received (hot-rolled) material condition was also employed for comparison. The crack propagation test results were summarized in terms of FCG rate (da/dN) versus stress intensity factor range (ΔK) curves. In order to describe the FCG behavior, two models were tested: the conventional Paris equation [16] and a new exponential equation developed for materials showing non-linear FCG behavior [17]. The results allowed correlating the tensile properties and crack growth resistance to the microstructural features. The discussions are supported by fractographic analyses via SEM. Moreover, it is shown that the Region II of FCG curves of the dual and multiphase microstructural conditions are better modeled by dividing them in two parts.

2. Experimental Procedure

The material used in this study was a commercial grade low carbon microalloyed steel, developed by CSN under the designation of RD480. The chemical composition of this steel is given in Tab. 1. The material was received as hot rolled plates with 5 mm in thickness, from which tensile and fatigue specimens were machined. These specimens were divided in four lots; the first one remained in the “as received” (AR) condition. The others were hold in furnace at 800, 950 and 1200°C for 30 min, and then the specimens were quenched directly into cold water. After heat treatment, cross-section of samples were polished, etched and observed under light and scanning electron microscope (SEM) in order to reveal their microstructures. Three distinct etching procedures were adopted: 2% nital, 10% sodium metabisulphite and a combination of them.

Table 1. Chemical composition of RD480 steel.

Element	C	Mn	P	S	Si	Cu	Ni	Cr
wt.%	0.085	1.169	0.017	0.005	0.053	0.007	0.008	0,016
Element	Mo	Sn	Al	N	Nb	V	Ti	B
wt.%	0.005	0.003	0.021	0.0055	0.035	0.003	0.013	0.001

The tensile and fatigue crack growth tests were conducted at room temperature in laboratory air using a MTS 810.23m servo-hydraulic machine with 250 kN capacity. For the tensile tests, small size specimens (6 mm in width and gage length of 30 mm) and a constant crosshead speed of 0.5 mm/min were employed.

Compact tension specimens, cut in the LT orientation, were adopted for the FCG tests. These were performed with constant load amplitude under force control at load ratio (min/max) $R = 0.1$. The test frequency was kept constant at 10 Hz and the loading waveform was sinusoidal. The compliance method of crack length monitoring was used during the tests and the five point incremental polynomial technique was employed for computing the crack growth rate. All of the experimental and numerical procedures were in conformity with the standard practice for Measurement of Fatigue Crack Growth Rates (ASTM E647-95a). The crack propagation test results were summarized in terms of FCG rate (da/dN) versus stress intensity factor range (ΔK) curves. The fracture planes of the fatigued specimens were examined using a scanning electron microscope (SEM) LEO 435 Vpi.

3. Results and Discussion

The obtained results are summarized in three sections: microstructural analysis, tensile propertied and fatigue crack growth behavior. In these analyses, the material in the "as received" condition is referred as AR; the remaining material conditions are designated by WQ (from "water quench") followed by a number representing the soaking temperature, i.e., WQ800, WQ950 and WQ1200.

3.1. Microstructural analysis

It can be seen if Fig. 1a that the AR material presents fine grained microstructure with polygonal morphology. The microalloying elements Nb, V and Ti contribute to the formation of small size grains in the hot rolled steel. Figure 1b (nital etching) shows that the main phases in this material are perlite (dark) and ferrite (bright). The same material condition was also etched in an aqueous solution of sodium metabisulphite in order to reveal the presence of retained austenite. However it was not possible to detect this phase, which means that its amount in the AR condition is negligible.

The microstructure of WQ800 condition, shown in Fig. 2, presented changes in grain size compared to the AR material. By heating the steel to the intercritical region (800°C), two phenomena occur: the formation of carbon-enriched austenite and the growth of non-transformed ferrite grains. The austenite grains in equilibrium with the remaining ferrite are small and in lower amount due to the low carbon content of the alloy. After quenching, austenite is transformed in a second, harder phase (martensite and/or bainite) spread over the ferrite matrix, resulting in a typical dual phase steel microstructure. In Fig. 2b, the same microstructure is revealed by sodium metabissulphite etching. In this case, the small white globular areas correspond to retained austenite, indicating that part of the austenite did not transform, due to the severity of the water quench.

It can be seen in Fig. 3a that the water quench from a total austenitization temperature (950°C) brought deeper microstructural changes to this steel. The polygonal aspect of the grains was reduced, the soft phase (ferrite) became more acicular and the amount of the second phase (martensite/bainite) is increased. The overall microstructure is still refined. Liang *et al.* [11] observed a similar microstructure as a result of water quenching from the austenitic region. The micrography obtained with sodium metabisulphite etching, Fig. 3b, shows that the amount of retained austenite (white phase) is increased for this soaking temperature.

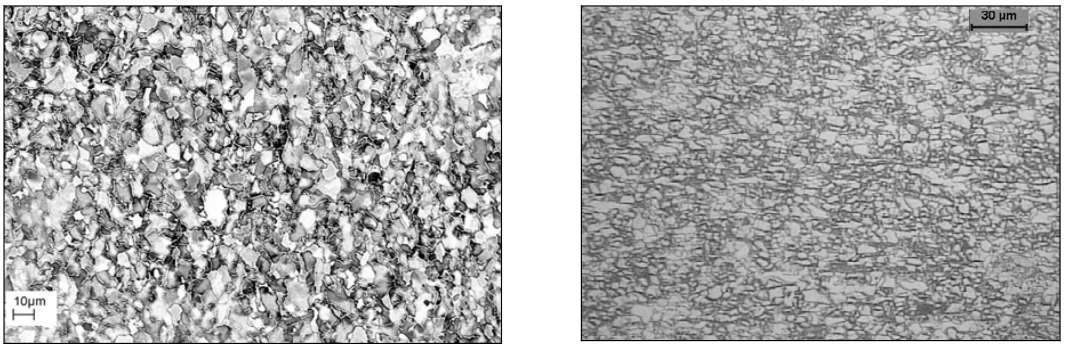

(a) (b)

Fig. 1. RD480 steel, AR condition. (a) SEM micrography showing grain refinement; (b) optical micrography revealing the grain boundaries and phases: perlite (dark) and ferrite (etchant: 2% nital).

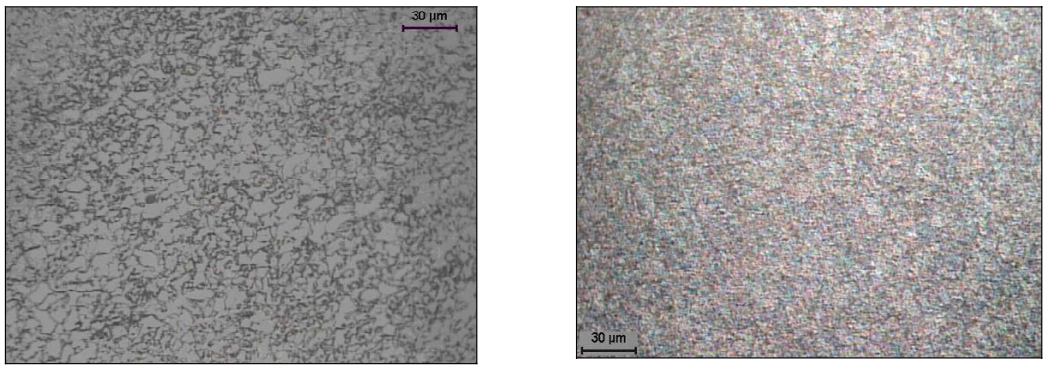

(a) (b)

Fig. 2. RD480 steel, WQ800 condition, optical micrographies. (a) dual phase structure (etchant: 2% nital); (b) retained austenite, white phase (etchant: 10% sodium metabissulphite).

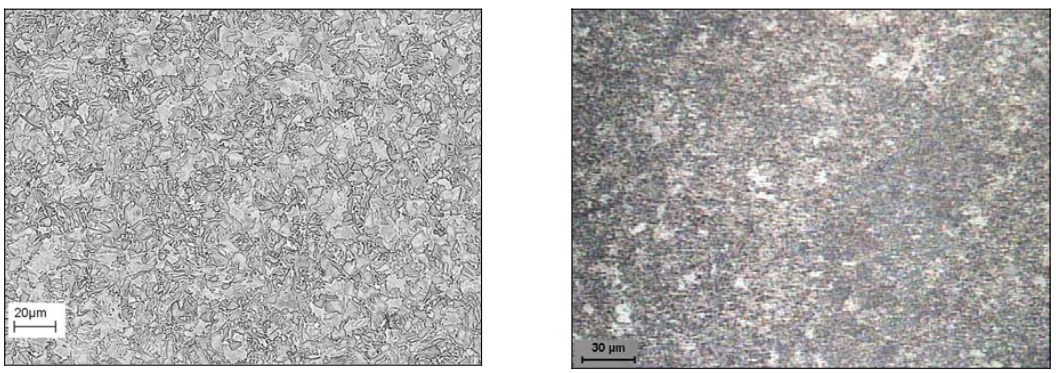

(a) (b)

Fig. 3. RD480 steel, WQ950 condition. (a) SEM micrography showing acicular ferrite and increasing in amount of the second phase; (b) optical micrography showing retained austenite, white phase (etchant: 10% sodium metabissulphite)

The microstructure of WQ1200 condition is shown in Fig. 4. In this case, the blue-tinted phase (martensite), sprinkled with a white phase (retained austenite), has a tendency to surround the ferritic phase (pale brown) like a net, see Fig. 4a. It can be seen in Fig. 4b the ripped up morphology of the transformed phases, indicating that shearing events occurred during transformation. This occurrence is well known for low carbon (less than 0.6 wt. pct.) steels.

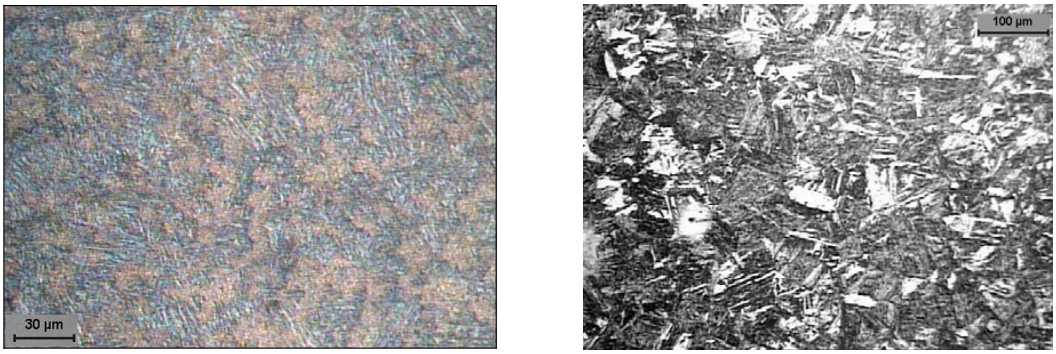

(a) (b)

Fig. 4. RD480 steel, WQ1200 condition, optical micrographies. (a) martensitic net (blue), sprinkled with retained austenite (white) and surrounded ferrite (pale brown); (b) ripped up morphology of the transformed phases (etchants: 2% nital and 10% sodium metabissulphite)

3.2. Tensile properties

The tensile properties are summarized in Tab. 2, where σy is the yield stress, σu is the ultimate tensile strength and ΔL is the percent elongation. The AR material exhibits a high ductility level due to its high ferrite content. The σy / σu ratio is also high, due to the hot rolling production process. The WQ800 material condition experienced an increase of about 20% in the tensile strength, compared to the AR material, and a decrease in the yield stress, while the elongation of 17% means that the ductility is kept in an acceptable level (for most of the automotive applications) due to the presence of the ferritic phase. The WQ800 condition shows also an important characteristic: the lowest σy / σu ratio among all the tested material conditions. It was shown that the steels with a σy / σu ratio below 0.68 are very suitable to applications embodying cold work processes [18]. The WQ950 condition presented increases in the yield stress and tensile strength, and a decrease in the percent elongation, which became critical once the necking was observed to begin at 5% total strain [15]. This behavior is related to the increases in the volume fraction of martensite and in the hardness of the ferritic phase, which assumed an acicular morphology (Fig. 3a). According to Gündüz [19], martensite is dominant in controlling the tensile properties, and a previous work by Stein et al. [20] showed that samples heat treated in the range 900-950°C presented refined martensite, due to the small growth of austenitic grains, with a low volume fraction of polygonal ferrite and significant amount of acicular ferrite. The highest σy and σu values were obtained for the WQ1200 condition. From Fig. 4a it can be concluded that the high cooling rate in this condition reduced the atomic diffusion to short circuits, resulting in a microstructure characterized by a martensitic net surrounding the ferritic grains. The tensile strength is increased due to this phase morphology and to the increase in the hardness of ferrite (which is more sheared), but the ductility suffers a huge drop.

Table 2. Tensile properties of RD480 steel with distinct microstructural conditions.

Condition / Property	σ_y (MPa)	σ_u (MPa)	ΔL (%)	σ_y / σ_u
AR	459	541	32	0.85
WQ800	343	649	17	0.53
WQ950	489	676	15	0.72
WQ1200	872	964	9	0.90

3.3. Fatigue crack growth (FCG) behavior

The FCG results in the range 10-8-10-6 m/cycle (Region II) for the as received material and for the heat treated conditions are shown in Fig. 5 with two tests in each condition. In this figure, a clear increase in the crack propagation resistance of the multiphase materials is observed. It can be stated that the formation of harder phases upon water quenching is responsible for this increase. In the heat treated conditions, the harder phases are spread over the softer ferritic matrix, thus creating a tendency if the crack to deviate from these phases and to propagate mainly through the ferrite, resulting in a more tortuous crack path. Besides, crack propagation through martensitic phase was also observed together with other mechanisms that contributed to increase the FCG resistance (Fig. 6). The lower resistance to crack propagation shown by WQ800 material when compared to the other heat treated conditions is probably due to the lower amount of ferrite in their microstructures (Figs. 2 to 4), which makes crack propagation through this phase more difficult to occur. Chen and Cheng [21] observed that the mechanical strength of dual and multiphase steels is higher when their microstructure is characterized by a martensitic phase surrounding ferrite islands. This feature was observed for WQ1200 condition (Table 2 and Fig. 4). The higher tensile strength of WQ1200 does not mean, necessarily, a better fatigue crack behavior as compared to the other heat treatments. This is clear when the FCG curves of WQ1200 condition is compared to those of WQ950 (Fig. 5). The complete surrounding of ferrite by harder phases, like observed for WQ1200 material, did not occur for WQ950. The phases morphology presented by WQ1200 resulted in high tensile strength, but lead to material embrittlement because the deformation of ferritic phase is inhibited (Fig. 7). This lack of ductility is probably behind the loss of fatigue crack growth resistance presented by WQ1200 when compared to WQ950.

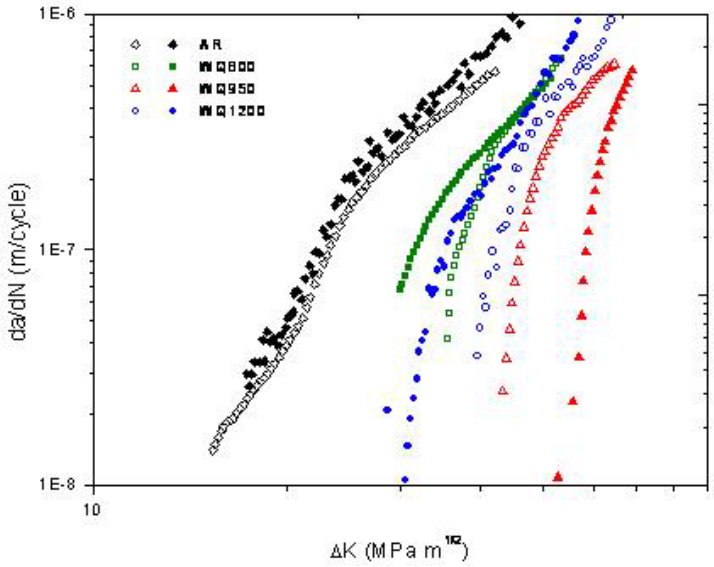

Fig. 5. Fatigue crack propagation curves of RD480 steel with distinct microstructural conditions.

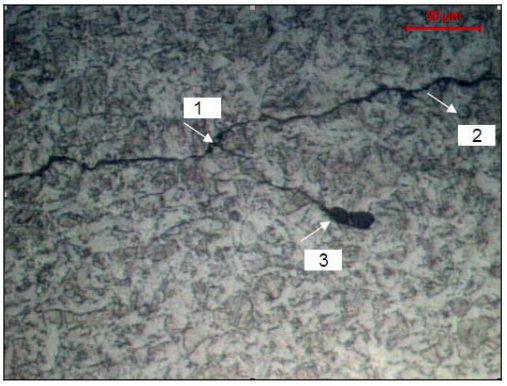

Fig. 6 . Fatigue crack path for WQ950 condition (1,000×): 1) crack bifurcation in martesitic phase, 2) crack deviation due to the presence of harder phases, 3) crack shielding by harder phase.

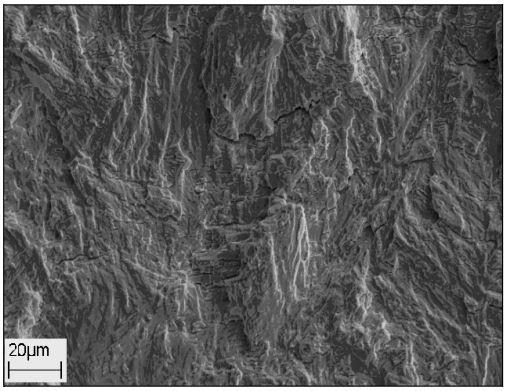

Fig. 7. Fatigue fracture surface of WQ1200 showing brittle mechanisms (1,000 ×).

In order to describe the FCG behavior of the multiphase alloys, two equations were tested: the conventional Paris model [16], given by Eq. (1), and a new exponential model developed for materials showing non-linear FCG behavior [17], given by Eq. (2).

$$\frac{da}{dN} = C(\Delta K)^n \tag{1}$$

$$\frac{da}{dN} = Ae^{(\beta/\Delta K)} \text{ , where } A = e^{\alpha} \tag{2}$$

In the exponential model, a calculation procedure is employed as follows: for each experimental point, a γ parameter is determined in the form of Eq. (3). By plotting the γ values against ΔK in the linear scale a straight line is obtained, for which the α and β values are respectively its slope and intercept.

$$\gamma = \ln\left(\frac{da}{dN}\right)\Delta K = \alpha\Delta K + \beta \tag{3}$$

Quantitative comparisons of these two models' performance can be done by the normalized sum of the squares of the residuals corresponding to the set of experimental points of each curve, which gives the average percent

deviation between the experimental and calculated growth rates. The calculated C and n values of Eq. (1) and α and β values of Eq. (2), as well as the percent deviations, are given in Tab. 3 for each material condition. Fig. 8, which shows the fatigue crack growth curves calculated according to these two models plotted together the experimental points for WQ 800 material condition, exemplifies the models behavior for all of the evaluated data sets**.**

Table 3. Fitting parameters for the Paris and Exponential models.

Material Condition	Paris Model			Exponential Model		
	C	*n*	% Deviation	α	β	% Deviation
WQ800 - 01	9.59×10^{-17}	5.75	0.16	-9.63	-239.8	0.12
WQ800 - 02	4.82×10^{-13}	3.56	0.078	-11.81	-135,54	0.045
WQ950 - 01	6.88×10^{-19}	6.71	0.30	-8.08	-334.9	0.26
WQ950 - 02	3.52×10^{-22}	8.29	0.052	-6.62	-529.31	0.047
WQ1200 - 01	5.05×10^{-17}	5.73	0.22	-9.44	-279.7	0.17
WQ1200 - 02	1.31×10^{-15}	5.04	0.139	-9.14	-259.62	0.199

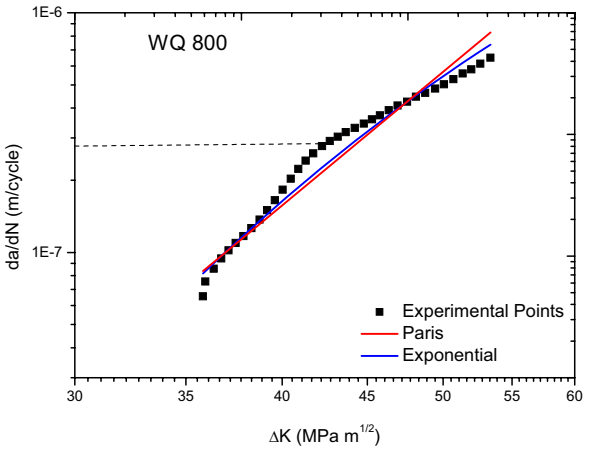

Fig. 8. FCG curve of WQ800 material, described by Paris and Exponential models.

From Fig. 8 and Tab. 3 it can be verified that the discrepancies between the models and experimental results for most of the tests are higher than the expected values for this kind of analysis [22]. Even the exponential equation, proposed for describing non-linear FCG behavior, was not successful in this case. However, a more careful observation of Fig. 8 clearly shows a change in the slope of the FCG curve. This change, defined here as the transition point, is indicated by a dashed line and occurs at a crack growth rate of 2.7×10^{-7} m/cycle, whatever the microstructural condition. Suzuki and McEvily [14] have already mentioned the existence of transition points in the FCG behavior of dual phase steels. These transitions were related to changes in crack path and in fracture mode due to a possible microstructural sensitivity of FCG behavior. Fig. 9 shows fracture surface aspects of WQ950 condition for crack lengths corresponding to FCG rates just below and above the transition point, respectively. In Fig. 9a it is possible to observe intense plastic deformation marks together with small dimples spread on the whole surface. These marks seem to be aligned at approximately 90° with FCG direction. After the transition point, Fig. 9b shows a decrease of the ductile fracture aspects, an increase in the deformation mark spacing and the existence of longer valleys with brittleness characteristics. Therefore, the Region II FCG curves of the dual and multiphase

microstructural conditions are better modeled by dividing them in two parts: above and below the transition point. Figs. 10–12 show, for one test of each material condition, the obtained results for both tested models. Tab. 4 presents the fitting parameters and the obtained percent deviation for the studied models. A comparison of the percent deviations shown in Tab. 4 with those of Tab. 3 allows concluding that the definition of a transition point resulted in a much better description of FCG behaviour for the multiphase steels. Moreover, there is no significant difference in the efficacy of the two models for both regions of the FCG curves. Another important observation is that the slopes of the FCG curves in the region above the transition point show the conventional behaviour of Region II FCG for all the material conditions, whereas the slopes of the regions below the transition point are very high, as if a threshold ΔK was being approached.

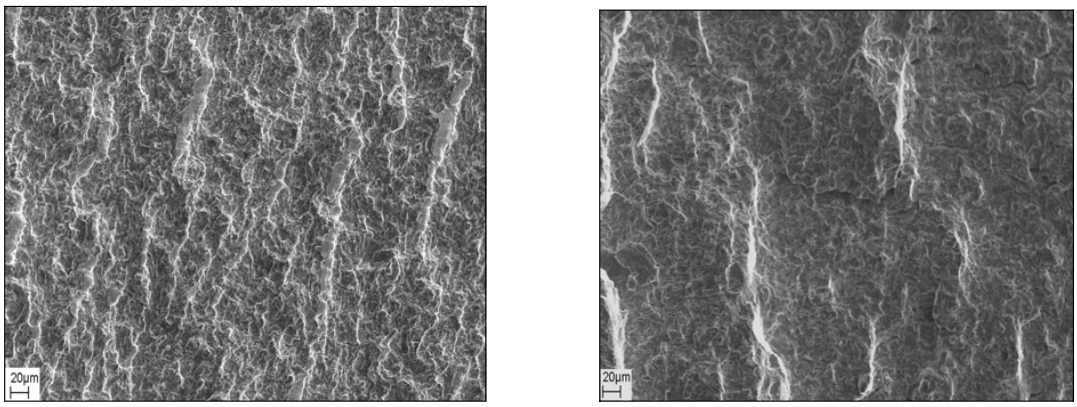

(a) (b)

Fig. 9. Fatigue crack surface of WQ950 (a) before and (b) after crack growth transition.

Table 4. Fitting parameters for the Paris and Exponential models considering the transition point.

Material Condition	Paris Model			Exponential Model		
	C	*n*	% Deviation	α	β	% Deviation
WQ800-01	2.22×10^{-22}	9.31	0.080	-6.60	-356.7	0.070
	5.32×10^{-13}	3.52	0.006	-11.04	-172.4	0.009
WQ800-02	2.94×10^{-15}	5.01	0.041	-10.87	-166.96	0.03
	7.75×10^{-12}	2.82	4.46×10^{-3}	-12.03	-125.85	0.012
WQ950-01	1.39×10^{-31}	14.30	0.063	-4.66	-525.9	0.057
	1.08×10^{-12}	3.19	0.030	-11.44	-182.4	0.020
WQ950-02	3.02×10^{-28}	11.68	0.021	-3.51	-722.04	0.019
	6.12×10^{-18}	5.97	1.24×10^{-3}	-8.59	-398.17	2.29×10^{-3}
WQ1200-01	9.66×10^{-26}	11.05	0.096	-4.97	-474.7	0.092
	2.75×10^{-13}	3.60	0.052	-10.78	-202.4	0.056
WQ1200-02	1.38×10^{-22}	9.59	0.068	-6.84	-328.57	0.06
	7.77×10^{-15}	4.59	0.051	-9.48	-247.77	0.1

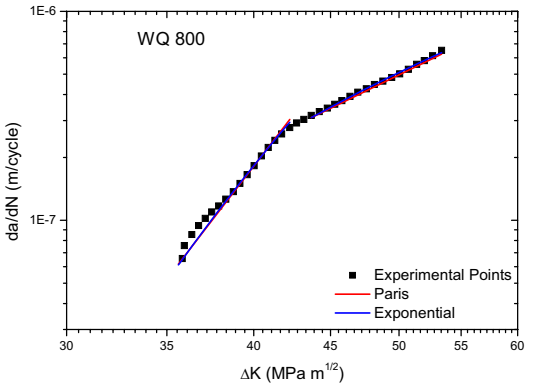

Fig. 10. Two regions of FCG curve of WQ800 material, described by Paris and Exponential models.

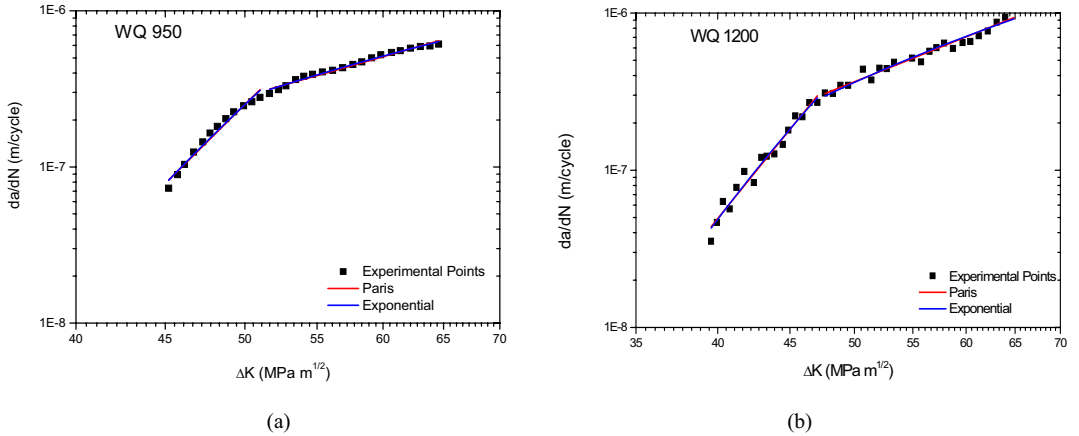

Figure 11. Two regions of FCG, described by Paris and Exponential models. a) curve of WQ950 material b) curve of WQ1200 material

4. Conclusion

From the presented results, the following can be concluded:

- Multiphase microstructures with distinct phase contents and morphologies are obtained by water quenching the microalloyed steel RD480 from different temperatures;
- Both the tensile strength and the FCG resistance of multiphase conditions have increased when compared to the properties of the AR material;
- Among the tested material conditions, the best FCG resistance was obtained by water quenching RD480 steel from 950°C, leading to a microstructure in with great amount of harder phases was present, although not enough to completely surround the softer phase (ferrite);
- A better description of the FCG behavior of RD480 steel with multiphase microstructures is obtained if the experimental curves are divided in two regions: above and below a transition point.

Acknowledgements

D. F. Laurito acknowledges CAPES for the grant.

References

[1] Misra RDK., Tenneti KK, Weatherly GC, Tither G. Microstructure and texture of hot-rolled Cb-Ti and V-Cb microalloyed steels with differences in formability and toughness. *Metallurgical and Materials Transactions A* 2003; **34**: 2341-51.

[2] Naylor DJ. Microalloyed forging steels. *Mater Science Forum* 1998; **284–2**: 83–93.

[3] ASM Handbook. Properties and selection: irons, steels, and high performance alloys. ASM International 1999; **1**.

[4] Matlock DK., Krauss G, Speer JG. Microstructures and properties of direct-cooled microalloy forging steels. *J. Mater Process. Technol* 2001; **117**: 324–8.

[5] Shanmugama S, Misra RDK, Mannering T, Panda D, Jansto SG. Impact toughness and microstructure relationship in niobium- and vanadium-microalloyed steels processed with varied cooling rates to similar yield strength. *Materials Science and Engineering* 2006; **437**: 436–445.

[6] Elisei CCA, Abdalla AJ, Hashimoto TM, Pereira MS. Utilização de metalografia colorida na identificação dos microconstituintes de um aço microligado**.** In: *Proceedings of the Congresso Brasileiro de Engenharia e Ciências dos Materiais*. Foz do Iguaçu: ABM, ABC, ABPol; 2006, p. 1–12.

[7] Anumolu R, Kumar RB, Misra RDK, Mannering T, Panda D, Jansto SG. On the determining role of microstructure of niobium-microalloyed steels with differences in impact toughness. *Materials Science and Engineering* 2008; **491**: 55–61.

[8] Abdalla AJ, Hashimoto TM, Moura NCM, Pereira MS, Souza NS, Mendes FA. Alterações das propriedades mecânicas em aços 4340 e 300M através de tratamentos térmicos isotérmicos e intercríticos. In: *Proceedings of the Congresso Anual da Associação Brasileira de Metalurgia e Materiais*. São Paulo: ABM; 2004, p. 1–10

[9] Maleque MA, Ponn YM, Masjuki HH. The Effect of intercritical heat treatment on the mechanical properties of AISI 3115 steel. *Journal of Materials Processing Technology* 2004; **153**: 482-7.

[10] Suleyman G. Static strain ageing behaviour of dual phase steels. *Materials Science and Engineering* 2007; **486**: 63–71.

[11] Liang X, Li J, Peng Y. Effect of water quench process on mechanical properties of cold rolled dual phase steel microalloyed with niobium**.** *Materials Letters 2008*; **62**: 327–9.

[12] Tayanç M, Aytaç A, Bayram A. The effect of carbon content on fatigue strength of dual- phase steels. *Materials & Design* 2007; **28-6**:1827-35.

[13] Baptista CARP, Voorwald HJC, Barboza MJR., Pastoukhov VA. Efeito de tratamentos térmicos intercríticos na propagação da trinca por fadiga em um aço de baixo carbono. In: *Proceedings of the 49º Congresso Internacional de Tecnologia Metalúrgica e de Materiais*. São Paulo: ABM; 1994, p. 127-38.

[14] Suzuki H, Mcevily AJE. Microstructural effects on fatigue crack growth in a low carbon steel. *Metallurgical Transactions A-Physical Metallurgy* 1979; **10-A**: 475-1.

[15] Laurito DF, Baptista CARP, Abdalla AJ, Oliveira MCA. Modifying the microstructure and mechanical properties of a microalloyed steel developed for use in the automotive industry. *SAE Technical Paper Series* 2009; **36**: 1-8.

[16] Paris P, Erdogan F. A Critical analysis of crack propagation laws. *J. Basic Engng., Trans. ASME* 1963; **85**: 528-34.

[17] Adib AML, Baptista CARP. An exponential equation of fatigue crack growth in titanium. *Materials Science and Engineering* 2007;**452-3**: 321-5.

[18] Abdalla AJ, Hashimoto TM, Pereira MS, Anazawa RM. Otimização das propriedades mecânicas de um aço ARBL através de tratamentos térmicos**.** In: *Proceedings of the Congresso Iberoamericano de Metalurgia e Materiales*. Habana: IBEROMET IX; 2006, p. 276- 81.

[19] Gündüz S. Static strain ageing behaviour of dual phase steels. *Materials Science and Engineering* 2008; **486**: 63–71.

[20] Stein CR. Efeito da rápida austenitização sobre as propriedades mecânicas de um aço SAE1045**.** *Rem: R. Esc. Minas* 2005; **58**: 51–6.

[21] Chen HC, Cheng GH. The effect of martensite strength on the tensile strength of dual phase steels. *Journal of Materials Science* 1989;**24**: 1991-4.

[22] Baptista CARP, Torres MAS, Pastoukhov VA, Adib AML. Development and evaluation of two parameter models of fatigue crack growth. In: *Proceedings of the IX International Fatigue Congress*. Atlanta: Elsevier; 2006, p. 1-10 (cd-rom).